(Preprint) AAS 11-482

EPOXI TRAJECTORY AND MANEUVER ANALYSES

Min-Kun J. Chung, Shyamkumar Bhaskaran, Steven R. Chesley, C. Allen Halsell, Clifford E. Helfrich, David C. Jefferson, Timothy P. McElrath, Brian P. Rush, Tseng-Chan M. Wang, and Chen-wan L. Yen*

The EPOXI mission is a NASA Discovery Mission of Opportunity combining two separate investigations: Extrasolar Planet Observation and Characterization (EPOCh) and Deep Impact eXtended Investigation (DIXI). Both investigations reused the DI instruments and spacecraft that successfully flew by the comet Tempel-1 (4 July 2005). For EPOCh, the goal was to find exoplanets with the high resolution imager, while for DIXI it was to fly by the comet Hartley 2 (4 Nov 2010). This paper documents the navigation experience of the earlier maneuver analyses critical for the EPOXI mission including statistical ΔV analyses and other useful analyses in designing maneuvers. It also recounts the trajectory design leading up to the final reference trajectory to Hartley 2.

INTRODUCTION

The EPOXI mission is a NASA Discovery Mission of Opportunity combining two separate investigations: Extrasolar Planet Observation and Characterization (EPOCh) and Deep Impact eXtended Investigation (DIXI). Both investigations reused the Deep Impact (DI) instruments and spacecraft launched on 12 Jan 2005. Deep Impact encountered the comet Tempel-1 on 4 July 2005, impacting with an impactor spacecraft for an investigation of the comet's nucleus and subsequently passing close by the comet with the flyby spacecraft.[1] For the EPOCh investigation, EPOXI used the DI HRI (high resolution imager) on the flyby spacecraft to find exoplanets starting in early 2008. For the DIXI portion of the investigation, the EPOXI spacecraft was tasked to encounter the comet Hartley-2 on 4 Nov 2010.

In this paper we focus primarily on the navigation experience of the earlier maneuver analyses leading up to the encounter.† We discuss maneuver analyses found important and useful for the mission including statistical ΔV analysis and other analyses in designing and, in some cases, canceling maneuvers. First, we recount the trajectory design leading up to the final reference trajectory selected for the Hartley 2 encounter.

TRAJECTORY DESIGN

Due to the fact that EPOXI was an extended mission with an already established initial trajectory and that the target was a comet with uncertain ephemerides, the reference trajectory needed

* Mission Design & Navigation Section, Jet Propulsion Laboratory, 4800 Oak Grove Dr., Pasadena CA 91109-8099
† There will be a separate paper focusing on the latter part of maneuver design near the encounter by Clifford Helfrich.

to be redesigned a few times. In this section we describe a few preliminary trajectories considered for the mission as well as the final reference trajectory selected for the encounter.

Trajectories described in this section were designed using Jet Propulsion Laboratory (JPL) section software: MIDAS for the initial guess and CATO for the final integrated trajectory.[2,3]

Preliminary Trajectory Design

Although the DI mission to Temple-1 was only 6 months in duration, the DI spacecraft was launched into a 1.5-year period orbit with respect to Sun, which allowed for a future Earth flyby after about 3 years, in expectation that some kind of extended mission would be possible. Soon after the Tempel-1 flyby on 20 July 2005, a Trajectory Correction Maneuver (TCM-8) of 97 m/s was performed to set the trajectory on course for an Earth flyby and eventually an encounter with comet Boethin.

Original Trajectory to Boethin. The extended mission officially began in June 2007 under the NASA Discovery Program as a Mission of Opportunity. On 25 Sep 2007 the spacecraft was awakened from hibernation to resume its operations and to perform TCM-9 of 1 m/s to set the course for an Earth Gravity Assist (EGA-1) on 31 Dec 2007 and ultimately what was expected to be an encounter with comet Boethin on 5 Dec 2008. (Refer to Figure 1 for the original trajectory to Boethin in blue.)

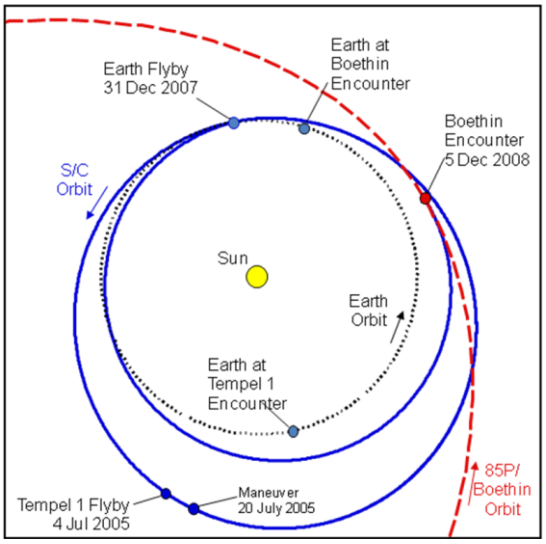

Figure 1. DI / EPOXI Trajectory to Boethin.

Much analysis of the effects of the ±2-σ uncertainty of the Boethin ephemeris was performed under the assumption that the comet might be recovered several months before the encounter in May 2008. However, the comet Boethin was not redetected in spite of many attempted observations. It may have in fact broken up.

Backup Trajectory to Hartley 2. Fortunately at the same time, analysis was also proceeding on developing a backup trajectory to comet Hartley-2. Due to the lack of a viable target for Boethin, the principal investigator Mike A'Hearn made a formal decision on 19 Oct 2007 to target Hartley 2, whose ephemeris was much better known. TCM-9 of 14.5 m/s was performed on 1 Nov 2007 to set the course for EGA-1 on 31 Dec 2007 and eventually for an encounter with the comet Hart-

ley 2 on 11 Oct 2010. The backup trajectory had two additional EGAs (EGA-2 and EGA-3). Refer to Figure 2 below for the backup trajectory to Hartley 2 in green. The dots represents 100-day intervals counting backwards from the encounter.

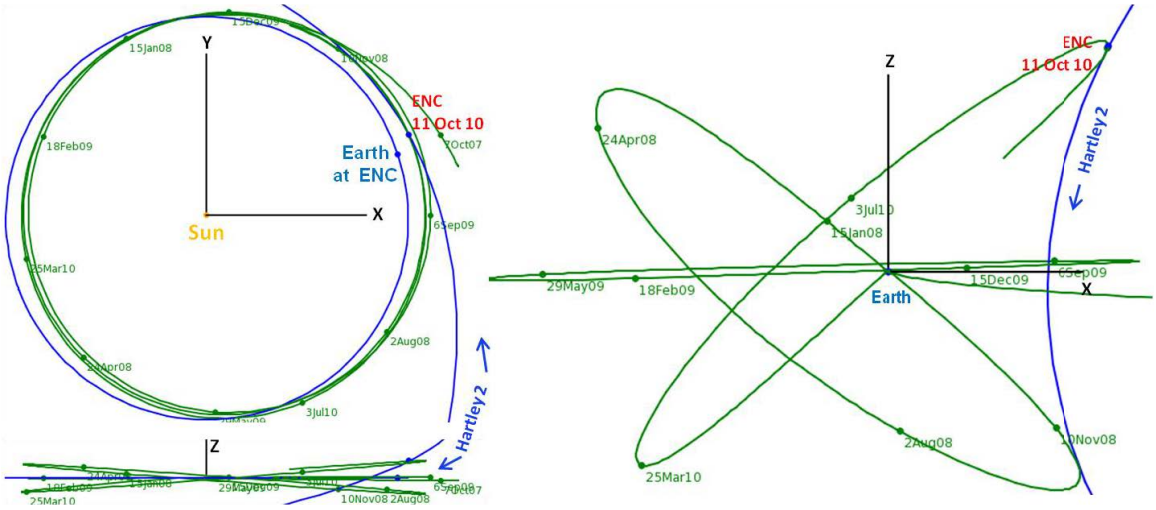

Figure 2. Backup Trajectory to Hartley 2 in Sun-Centered EMO2000 Top and Side View (Left) and Earth-Centered Sun-Earth Rotating Frame Side View (Right).

A large concern for the mission was a low Sun-comet-spacecraft phase angle at the encounter. The backup trajectory had an approach phase angle of only 70º, whereas a phase angle of about 90º was preferred for the Infrared (IR) spectrometer to remain cooler on approach.

Other Proposed Trajectories to Hartley 2. Efforts were made to improve on the approach phase angle of the original backup trajectory in early 2008. Motivated by a possibility for a proposal to observe an Earth flyby anomaly, an attempt was made to insert a very close Earth flyby.[4] By making the trajectory leg prior to the last Earth flyby into a six-month Earth loop, an alternate trajectory was found that yielded a much better approach phase angle of 85º in addition to the close Earth flyby.[*] However, the very close Earth flyby contained an Earth eclipse too long for the spacecraft's survival on battery power. Although this trajectory was not ultimately selected due to the long eclipse, it provided insight toward the right direction to pursue.

Final Reference Trajectory to Hartley 2

By preserving the trajectory leg from the last Earth flyby (EGA-3) to the comet encounter in the previous design, but converting the intermediate trajectory leg from EGA-2 to EGA-3 into a 1.5 year loop with two distant Earth flybys (DFB-1 and DFB-2), one in every six months, a final solution was determined that also had a favorable approach phase angle of 86º but without Earth eclipse issues.[†] This was achieved by a relatively large initial maneuver[‡] (TCM-12 of 31.5 m/s) to

---

[*] This alternate trajectory was found by Timothy P. McElrath.

[†] The final reference trajectory as well as the backup trajectory was found by Chen-wan Yen.

[‡] The initial design contained two deterministic ΔVs before EGA-2 to minimize the ΔV; however, due to the EPOCh observation earlier in 2008 as well as the ΔV cone constraint, the two were combined into one. The ΔV cone constraint is defined and discussed further in the "Avoiding Vectorization of TCM" subsection of the OTHER MANEUVER DESIGN ANALYSES section.

to set EGA-2 such that the trajectory leg until EGA-3 remained in a narrow vertical region pointed towards Ecliptic north and south of Earth. This kept the Sun range approximately 1 AU for thermal reasons (the backup trajectory went below 0.885 AU while above 0.88 AU was the S/C requirement). It was necessary to insert a small deterministic maneuver, TCM-18, before EGA-3 to allow CATO to converge targeting comet Hartley 2. The target B-plane parameters were **B•T** of -77.4 km and **B•R** of 695.8 km, 700 km away from the comet center.*

This final reference trajectory contained two additional EGAs (EGA-2 and EGA-3) as well as two distant Earth flybys (DFB-1 and DFB-2). Refer to Figure 3 below for the final reference trajectory plot in Earth-centered, Sun-Earth rotating frame (side view from the Ecliptic) and Figure 4 below for the plot in Sun-centered EMO2000 frame (both top and side views from the Ecliptic). The green portion is from the backup trajectory; TCM-12 marks the beginning of the final reference trajectory in red. All executed TCMs are placed in the trajectory plot along with their execution date and ΔV magnitudes. Note that TCM-10, 11, 15, and 17 were canceled.

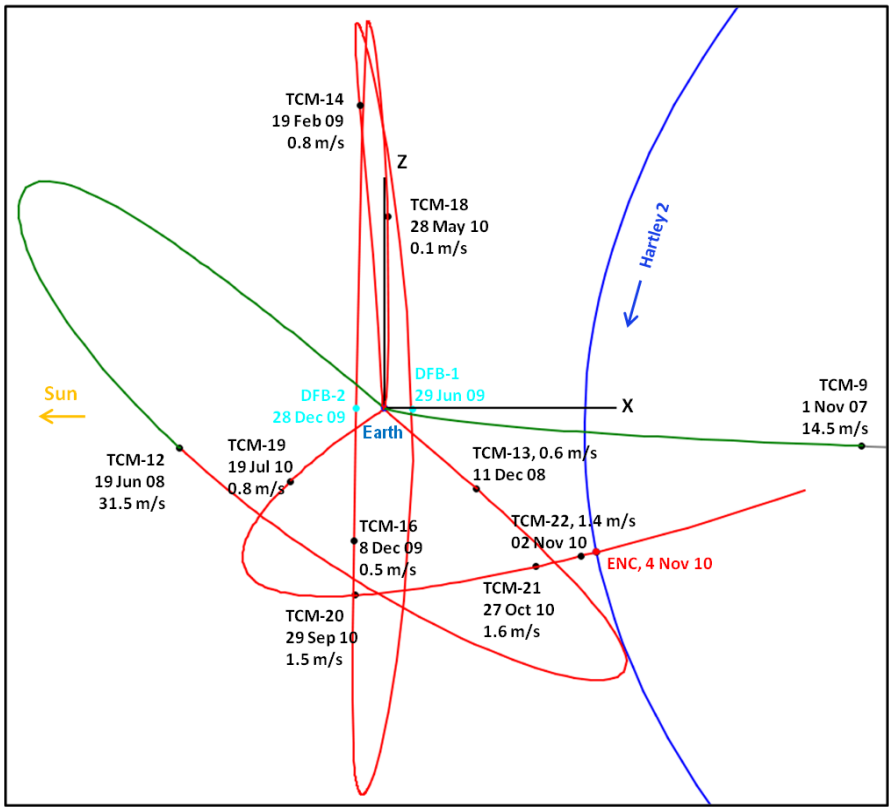

Figure 3. Final Reference Trajectory to Hartley 2 in Earth-Centered, Sun-Earth Rotating Frame.

* The flyby miss vector **B** is a vector from the comet center to the point where the incoming v-infinity vector direction **S** of the spacecraft penetrates the plane normal to **S**. **B•T** is the component along the **T**, which is normal to **S** and parallel to the Earth Mean Equator and Equinox of 2000 (EME2000). **B•R** is the component along the **R** = **S** x **T**.

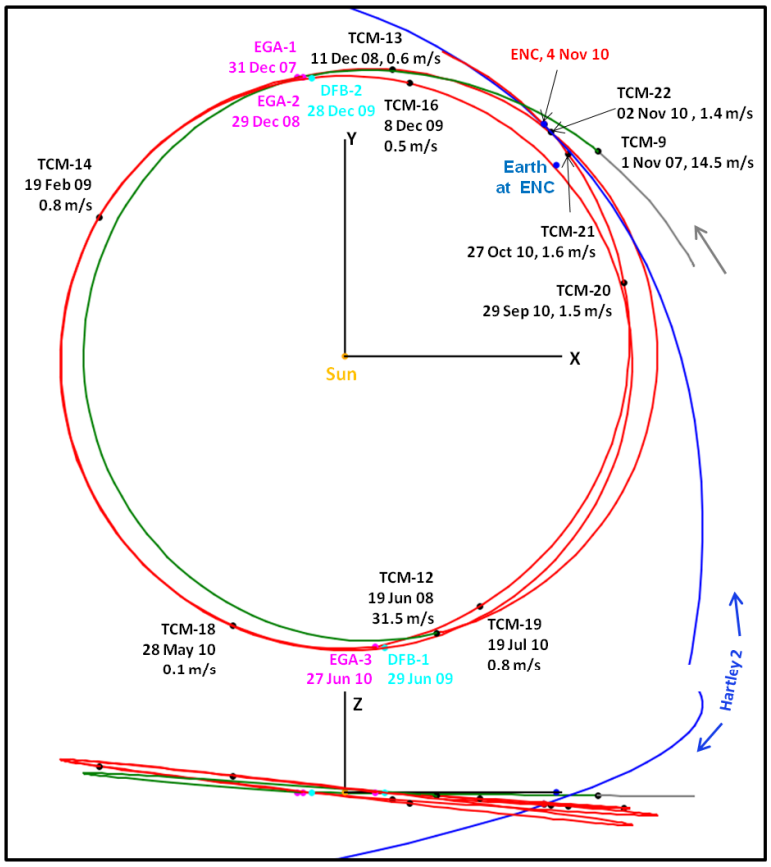

Figure 4. Final Reference Trajectory to Hartley 2 in Sun-Centered EMO2000.

STATISTICAL ΔV ANALYSIS

As shown above, the reference trajectory became more complex due to the increased number and magnitude of maneuvers. In the beginning of the EPOXI mission, the spacecraft had an estimated 19.7 kg of fuel remaining, of which 16.8 kg was allocated for maneuvers with respect to the initial Boethin trajectory (shorter than the final Hartley 2 trajectory). This amounted to 70.8 m/s of ΔV allocated for maneuver. When the target comet switched to Hartley 2, 14.5 m/s was consumed for TCM-9, leaving only 56.3 m/s remaining for maneuvers. When the reference trajectory was finally determined with a TCM-12 of 31.5 m/s (leaving only 24.8 m/s of margin), the project had to ensure that there was enough fuel or ΔV capability left on-board to complete the mission. This task was achieved by applying the statistical ΔV analyses at various points in the mission to ensure the spacecraft had enough ΔV remaining.

A brief introduction is given to the topics of orbit determination (OD) covariance and Monte Carlo simulation using OD covariances before we present a statistical analysis case.

OD Covariance

The OD analysts provide the maneuver analysts with OD covariances to be used in the statistical analyses. The OD covariances consist of the correlated covariance matrix for the spacecraft state,

determined at the time of the data cutoff (DCO) for each maneuver and mapped to the next significant encounter event such as an intermediate Earth flyby or the final Comet flyby.

For covariance analyses, an OD analyst begins by simulating Doppler and range radio data and optical navigation data.* These simulated data and the latest trajectory are input into a standard filter to estimate the spacecraft state, values for the maneuvers inside the data arc, and also the comet ephemeris when mapping to the comet flyby. Assumptions were made regarding the schedule of radio and optical navigation data, the number and timing of desaturation maneuvers (desats),† and the *a priori* uncertainties of all estimated or considered parameters (for example, the spacecraft and comet states, the maneuver parameters, desats, and solar radiation pressure). The filter estimates the spacecraft state throughout the data arc and maps this state and its uncertainty to the next encounter event. Refer to Reference 5 for an overview of EPOXI OD process.[5]

Monte Carlo Simulation Using OD Covariance

An initial sample state is obtained as an offset from the OD solution (which is the initial observed state) by sampling an OD uncertainty from the initial OD covariance (ODCZERO) that maps the uncertainty from the time of the OD solution to a future target event. Refer to Figure 5 below for a simplified diagram of OD covariance propagation. At DCO of the first maneuver, the initial sample state becomes the observed state for the first maneuver. The commanded ΔV is computed to shift the observed state to the desired state according to the specified maneuver optimization strategy. The actual ΔV, which is the commanded ΔV plus an execution error randomly sampled according to an execution error model (Gates model is used in EPOXI analysis),[6] is executed to shift the observed state toward the desired state. The shifted observed state $\boldsymbol{\Psi}'$ is computed by

$$\boldsymbol{\Psi}' = \boldsymbol{\Psi} + K \bullet \Delta \mathbf{V}_A$$

where $\boldsymbol{\Psi}$ is the initial observed state, K is the K-matrix, and $\Delta \mathbf{V}_A$ is an actual ΔV. A K-matrix $K(t, t_0)$ at time t is computed by

$$K(t, t_0) = \partial \boldsymbol{\Psi} / \partial \mathbf{X} \bullet \boldsymbol{\Phi}(t, t_0)$$

where $\partial \boldsymbol{\Psi} / \partial \mathbf{X}$ is the partial of the encounter (B-plane) state with respect to the Cartesian state transition matrix from t_0 to t.‡ A sample state for the second maneuver is obtained by sampling from the OD covariance of the first maneuver. This sampled state becomes the observed state at DCO of the next maneuver. If there is a change in the target for the next TCM, the sample state is mapped from the current target to the next target. The mapped state $\boldsymbol{\Psi}''$ is computed by

$$\boldsymbol{\Psi}'' = K_{\text{Next Target}} \bullet K_{\text{Current Target}}^{-1} \bullet \boldsymbol{\Psi}'$$

where $\boldsymbol{\Psi}'$ is the shifted state, $K_{\text{Next Target}}$ is a K-matrix mapped to the next target, and $K_{\text{Current Target}}^{-1}$ is an inverse of K-matrix mapped to the current target.

---

* For the initial predictions of future maneuvers, the OD process would be similar except that real radio and optical data would be used.

† Desats were much more frequent than pre-launch prediction (p. 40, Reference 1).

‡ The legacy JPL section software SEPV (a part of ODP) can write a K-matrix file when a maneuver search is converged. SEPV is a trajectory target search program.

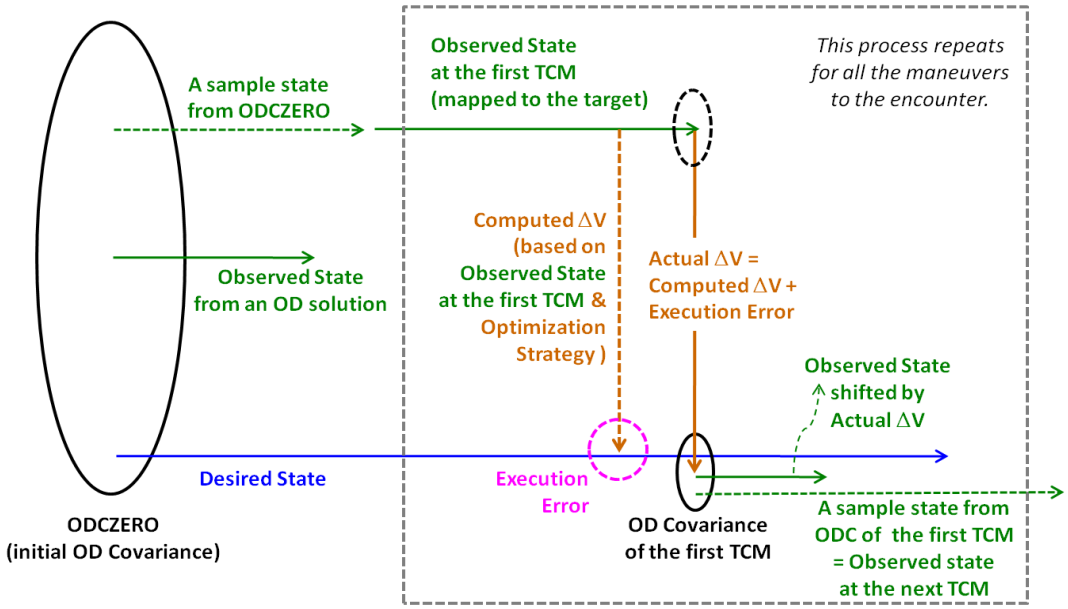

Figure 5. A Simplified OD Covariance Propagation Diagram.

This cycle repeats until all the maneuvers are accounted for and the sample state reaches the final encounter target. The above process is repeated for at least 5,000 randomly independent cases. Then the statistics of the actual ΔVs are gathered together to yield the mean, the sigma, and the expected percentile values of each individual TCM as well as the total TCMs. JPL Mission Design and Navigation Section software LAMBIC (Linear Analysis of Maneuvers with Bounds and Inequality Constraints) was used to perform the statistical ΔV analyses.[7] LAMBIC assumes linearity about the reference trajectory (valid for the EPOXI trajectory).

Using LAMBIC, we performed extensive statistical ΔV analyses at various points and at least once prior to each major reference trajectory update to ensure that ΔV statistics for the updated trajectory were acceptable at least at a ΔV95 (95% confidence) level. For example, at the final reference trajectory update prior to TCM-12, we had about 56 m/s ΔV capability allocated for maneuver. Using LAMBIC, we estimated ΔV95 for the final reference trajectory to be 47 m/s optimally or at most 53.5 m/s in the worst condition (vectorization for all future maneuvers), with the delivery dispersion up to 5 to 6 km at 1-σ in **B•R** and **B•T**. Thus, we were able to conclude that the fuel allocated for maneuver was sufficient to complete the entire mission at least with a ΔV95 confidence level.

Estimating and Considering the Comet Ephemeris Uncertainty*

Here we present a sample statistical analysis case done over a year before the encounter to ensure the ΔV budget was sufficient to complete the mission. Two different ways of reckoning the Hartley 2 ephemeris uncertainty were compared: (1) estimating the Hartley 2 ephemeris and un-

* Here "estimating" and "considering" are used in reference to the OD filter. Estimating a parameter means allowing its value to be adjusted in the filter, while considering a parameter means to incorporate *a priori* error to make the final OD uncertainty more realistic. Refer to "Filter" subsection in Reference 5 (p. 5) for more details.

certainty at TCM-19 and (2) considering only the Hartley 2 uncertainty at TCM-20 via an *a priori* comet covariance. These cases were necessary to work with a limitation in the LAMBIC program, which cannot separate the effects of both spacecraft state and target uncertainties at the same time. We wanted to confirm that both ways yielded satisfactory results. The two different ways were simulated by sampling two different sets of OD covariances.

OD Covariances Used for the Analysis. Table 1 below lists a set of OD covariances used in the statistical ΔV analysis with a particular OD solution numbered 225. One OD covariance is assigned for each TCM except for TCM-19 and 20. For TCM-19 and 20, two different OD covariances are assigned.

Table 1. Sample OD Covariances Used with the OD Solution #225.

TCM	OD Covariance name	DCO (days)	Maps to	σ(**B•R**) (km)	σ(**B•T**) (km)	Remark
-	ODCZERO		DFB-2	2355	6476	Initial OD covariance
16	ODC16	-10	DFB-2	39	36	Uncertainty mapped from DCO
17	ODC17	-10	EGA-3	806	1184	"
18	ODC18	-10	EGA-3	61	55	at EGA-3 – 40d
19	ODC19A	-10	ENC	6119	925	Estimate Hartley 2 ephemeris
	ODC19B			325	531	Not estimate Hartley 2 ephemeris
20	ODC20A	-10	ENC	147	139	Estimate Hartley 2 ephemeris
	ODC20B			6118	771	Consider Hartley 2 ephemeris uncertainty *a priori*
21	ODC21	-4	ENC	26	14	at ENC – 10d
22	ODC22	-2	ENC	8	10	at ENC – 4d

ODC19A pairs with OCD20A while ODC19B with ODC20B. The former pair estimates the Hartley 2 ephemeris uncertainty at TCM-19 and propagates the uncertainty forward to TCM-20, while the latter pair delays estimating the Hartley 2 ephemeris uncertainty until TCM-20, where it is dealt *a priori*. Note that the uncertainties decrease from ODC19A to ODC20A, yet it increases from ODC19B to 20B.

To clarify the latter pair further, ODC20B is an OD covariance that contains the *a priori* Hartley 2 ephemeris uncertainty at TCM-20 to determine the observed state at TCM-20. Although its uncertainty is large, the observed state will be fully resolved via optical observation at TCM-20.[8] Thus, its information can be used for the computation of the commanded ΔV at TCM-20. OCD20A is simply a normal OD covariance that estimates the states and propagates the uncertainty at TCM-20. This OD covariance is not to be used for the computation of the commanded ΔV at TCM-20. Its uncertainty is to be used to sample for the observed state of the next TCM, namely TCM-21. Figure 6 below depicts the two OD covariance pairs pictorially.

We wanted to confirm that the former pair indeed returned a good result by actually performing and comparing to the latter pair, which is closer to what was expected with the introduction of optical navigation near the time of TCM-20.

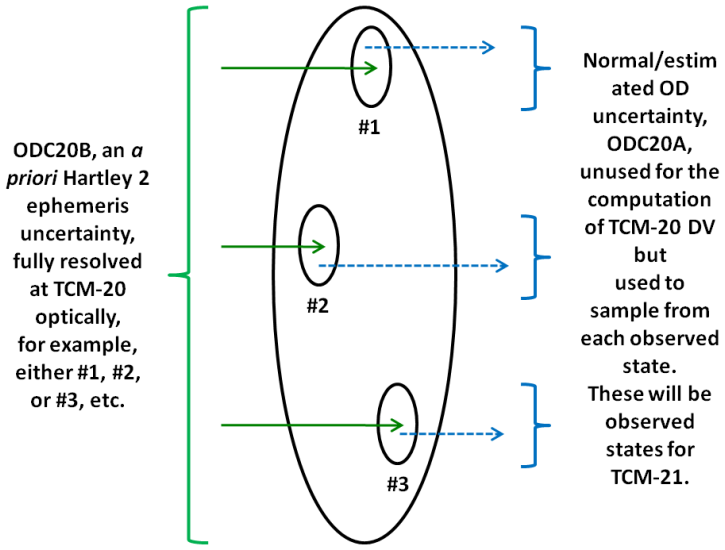

Figure 6. ODC20B: an *A Priori* Hartley 2 Ephemeris Uncertainty.

Result Estimating the Comet Ephemeris Uncertainty at TCM-19. The former pair (ODC19A at TCM-19 and OCD20A at TCM-20) yielded an expected result as shown in Table 2 below.

Table 2. Statistical ΔV Estimating the Comet Ephemeris at TCM-19.

TCM	Mean (m/s)	1-σ (m/s)	ΔV90 (m/s)	ΔV95 (m/s)	ΔV99 (m/s)	OD Covariance Used	Remark
16	0.73	0.54	1.49	1.77	2.31	ODC16	ODCZERO Used initially
17	0.09	0.06	0.17	0.22	0.31	ODC17	
18	0.45	0.30	0.87	1.03	1.36	ODC18	
19	4.20	2.49	7.34	8.65	12.09	ODC19A	Estimate Hartley 2 Ephemeris
20	2.35	1.74	4.79	5.71	7.51	ODC20A	
21	0.42	0.25	0.77	0.91	1.19	ODC21	
22	0.44	0.31	0.88	1.04	1.38	ODC22	
Total	8.69	3.18	12.77	14.34	18.10		

Result Using an A Priori Comet Ephemeris Uncertainty at TCM-20. However, when an *a priori* OD covariance was entered for TCM-20 (ODC20-ConEph), the ΔV results were unacceptably large (about 43 m/s at ΔV99 and 34 m/s at ΔV95). The result was due primarily to the LAMBIC limitation described above. However, by "rewiring" the part of LAMBIC that propagates the OD covariance, we were able make it handle an *a priori* OD covariance correctly. Figure 7 depicts an *a priori* OD covariance propagation.

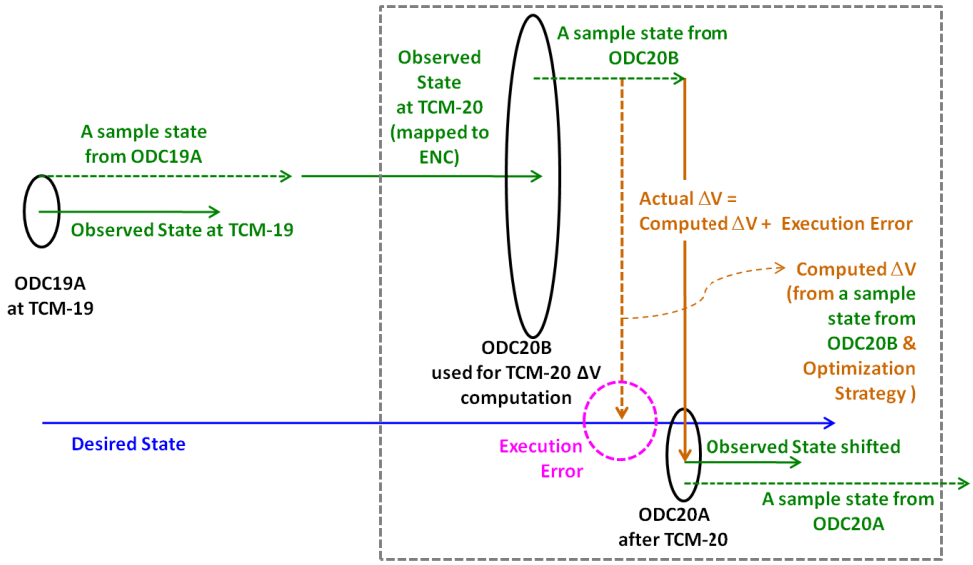

Figure 7. OD Covariance ODC20B Treated A Priori for TCM-20 ΔV Computation.

Table 3 shows the result obtained by using the latter pair (ODC20B *a priori* at TCM-20 as outlined above). The ΔV requirement of the uncertainty of the Hartley 2 ephemeris being resolved only at the time of TCM-20 via the availability of optical navigation, is only slightly larger than that of estimating the Hartley 2 ephemeris uncertainty at TCM-19 and propagating the uncertainty forward.

Table 3. Statistical ΔV Considering an *A Priori* Covariance at TCM-20.

TCM	Mean (m/s)	1-σ (m/s)	ΔV90 (m/s)	ΔV95 (m/s)	ΔV99 (m/s)	OD Covariance Used	Remark
16	0.73	0.54	1.49	1.77	2.31	ODC16	initial ODCZERO
17	0.09	0.06	0.17	0.22	0.31	ODC17	
18	0.45	0.30	0.87	1.03	1.36	ODC18	Pre-EGA-3
19	4.20	2.49	7.34	8.65	12.09	ODC19B	
20	2.36	1.74	4.81	5.73	7.52	OCD20A	ODC20B added *a priori*
21	0.42	0.25	0.77	0.91	1.19	ODC21	
22	0.44	0.31	0.88	1.04	1.38	ODC22	
Total	8.69	3.18	12.78	14.34	18.14		

Canceling a TCM via Statistical Analysis

The statistical analysis can be used to cancel a statistical TCM. Due to the delay of TCM-14 by a month to 19 Feb 2009 (between the original TCM-14 and TCM-15 times), TCM-15 was canceled. We ran statistical analysis without TCM-15 and found no impact on the ΔV requirement.

OTHER MANEUVER DESIGN ANALYSES

Given an OD solution by an OD analyst, a maneuver analyst designs the maneuver. This process may continue for several iterations as we observe the stability of the OD and maneuver solutions. When the DCO date nears, a stable OD solution is selected by the navigation manager to design the maneuver. The maneuver is designed and verified in the following steps:

(1) Check the OD solution by propagating and comparing with the no maneuver solution.

(2) Estimate the magnitude of the maneuver based on an impulsive model and deliver the magnitude to the Attitude Control System (ACS) team. ACS delivers the thrust and mass flow rate of the burn.

(3) Design the maneuver based on a finite model using the information from ACS. Deliver the finite burn information such as the start time, magnitude, and pitch angles to the ACS team. ACS delivers the burn implementation parameters.

(4) Verify the parameters by implementing the burn.

There was a small limitation in verifying the MIF due to a small difference in thrust modeling; our software did not model the actual thrust tapering, which is particular to the thrusters on the EPOXI spacecraft. Nevertheless, according to past experience, if we could correct the target difference by a trivial amount of ΔV (usually at the mm/s level), everything would be fine.

Updating the Reference Trajectory

Each time before a maneuver design, the reference trajectory was reoptimized in CATO to minimize the total ΔV. For the CATO run, force models were set similar to the settings in the legacy Orbit Determination Program (ODP) as much as possible. The CATO run yielded the intermediate targets for SEPV.* The final comet encounter target remained fixed. This process ensured the minimum ΔV.

Avoiding Vectorization of TCM

The EPOXI spacecraft had a ΔV direction constraint for thermal reasons. The solar panel normal vector (+Y-axis in the spacecraft frame) was required to be within 65° of the Sun. Refer to Figure 8 below for the diagram of the thermal constraint.

When an optimum maneuver violates this constraint, the nominal procedure would be vectorizing the maneuver into two burns in sequence in two consecutive days. Unfortunately, the optimum TCM-12 happened to violate this constraint, and thus it had to be vectorized. There were two disadvantages in vectorization. First, the program written to vectorize did not always produce an optimum result, thus, requiring more ΔV usage than necessary. As our ΔV budget was rather tight, this was not a good choice. Second, the vectorization added to operational complexity.

The easiest solution would have been to use a trajectory optimizer that already implements such a maneuver cone constraint. Unfortunately, CATO did not support such a constraint.

---

* We used the legacy JPL section program, SEPV, to search the ΔVs necessary to target the Hartley 2. For a longer trajectory, SEPV required intermediate targets. The new navigation software set was employed only several months before the encounter; however, the legacy software was operational in parallel to the end of mission as a backup and for a comparison purpose.

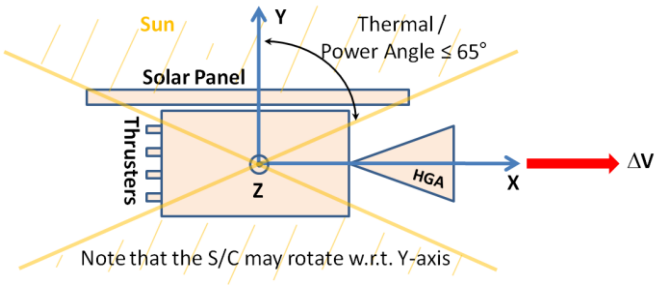

Figure 8. Thermal / Power Angle Constraint on ΔV.

The next best quick solution was writing a simple script to drive CATO. The driver script set up a small optimization problem using NPOPT[9] with only two controls: (1) the azimuth on the surface of the 65° constraint cone for TCM-12 (to ensure the thermal angle stays at 65° to take the full advantage without violating the constraint but only to search for the best azimuth) and (2) the magnitude of TCM-12 ΔV. The cost function was TCM-13 ΔV magnitude with a goal to drive it to zero. For each iteration, the driver ran CATO once with the TCM-12 ΔV specified by the two control variables to find the TCM-13 ΔV magnitude, while it minimized the total ΔV. Since we were using a numeric partial for NPOPT, the cost partials with respect to the two controls added two extra CATO runs per iteration; however, the problem was manageable since each CATO run took only several seconds. This capability gave us a way of implementing a single maneuver solution even when the thermal constraint was violated. The maneuver optimized in this way increased ΔV usage only by a few percent in comparison to the most optimum burn. Ultimately we did not have to vectorize any TCM for the whole mission.

ΔV Contour Map

For the EPOXI mission, since the ΔV requirement was one of the major factors in determining whether or not to cancel a TCM, it was helpful to visualize OD solutions and their uncertainty ellipses over a ΔV contour map whose axes are B-plane targets (X-axis is **B•T** and Y-axis is **B•R**) of the upcoming flyby (either of the Earth or the comet).

For example, Figure 9 below shows the contour map (at EGA-1 B-plane) of the total ΔV required to complete the mission to Hartley 2 with the backup trajectory without TCM-10. Several 1-σ delivery ellipses from different OD solutions are overlaid. Such a plot played a role in determining TCM-10 cancelation criteria. Since the OD solutions near the TCM-10 DCO were relatively stable around the red square (where TCM-10 targeted), and the 1-σ uncertainty ellipse did not extend much beyond the total ΔV of 16 m/s (for the backup trajectory to Hartley 2), it was recommended to cancel TCM-10.

Such ΔV contour plots were generated with future TCMs in an upcoming flyby target B-plane. They were also useful for the TCMs near the encounter in the Hartley 2 target B-plane.

Maneuver Solution With or Without a TCM

Another analysis that turned out useful in determining TCM cancelation criteria was running maneuver solutions with and without the TCM in question for several OD solutions. For those TCMs that we could cancel, usually we would observe a consistent pattern where the maneuver solutions without a TCM affect the next TCM very minimally. Often the next TCM ΔV would be very small (on the order of what the OD uncertainty would incur). This kind of analysis was helpful in determining to cancel TCM-11, 12, and 17.

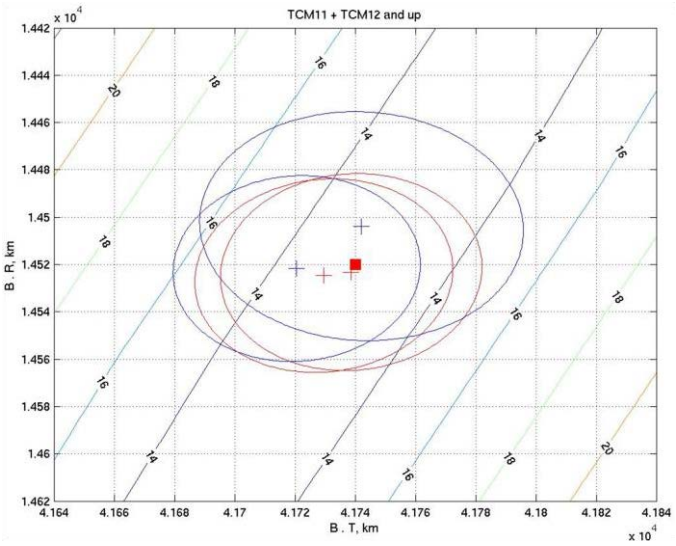

Figure 9. ΔV Contour Map at EGA-1 B-Plane without TCM-10, Overlayed with Several Delivery Ellipses from Different OD Solutions.

CONCLUSION

Due to a few updates to the reference trajectory design to improve the encounter condition as well as the comet ephemeris uncertainty, statistical ΔV analyses had to be performed at various times to ensure that we had enough ΔV to complete the mission. Thermal constraints required implementing a ΔV cone constraint that was solved by driving operations software with an optimizer. Strategies were developed to address these challenges and perform maneuver design efficiently with much automation, which led to a successful Hartley 2 encounter.

ACKNOWLEDGMENTS

This work was carried out at the Jet Propulsion Laboratory (JPL) of the California Institute of Technology under a contract with the National Aeronautics and Space Administration. The work was supported by the EPOXI project at JPL. Authors thank Roby S. Wilson, Raymond B. Frauenholz, and Laureano A. Cangahuala of JPL for their review of the paper.

REFERENCES

[1] R. B. Frauenholz, R. S. Bhat, S. R. Chesley, N. Mastrodemos, W. M. Owen Jr., M. S. Ryne, "Deep Impact Navigation System Performance," *Journal of Spacecraft and Rockets*, Vol. 45, No. 1, January-February 2008.

[2] C. G. Sauer, "MIDAS: Mission Design and Analysis Software for the Optimization of Ballistic Interplanetary Trajectories," *The Journal of the Astronautical Sciences*, Vol. 37, No. 3, 1989, pp. 251-259.

[3] D. V. Byrnes and L. E. Bright, "Design of High-Accuracy Multiple Flyby Trajectories Using Constrained Optimization," *AAS/AIAA Astrodynamics Specialist Conference*, Halifax, Nova Scotia, Canada, Paper 95–307 (August 1995).

[4] J. D. Anderson, J. K. Campbell, J. E. Ekelund, *et al*., "Anomalous Orbital-Energy Changes Observed during Spacecraft Flybys of Earth," *Physical Review Letters*, 100.9 (2008).

[5] S. Bhaskaran, M. Abrahamson, S. Chesley, M. Chung, A. Halsell, R. Haw, C. Helfrich, D. Jefferson, B. Kennedy, T. McElrath, W. Owen, B. Rush, J. Smith, T. Wang, C. Yen, "Navigation of the EPOXI Spacecraft to Comet Hartley 2," *AAS/AIAA Astrodynamics Specialist Conference*, 2011 AAS/AIAA Meeting Paper (submitted for publication).

[6] C. R. Gates, "A Simplified Model of Midcourse Maneuver Execution Errors", JPL Technical Report 32-504, 15 October 1963.

[7] E. H. Maize, "Linear Statistical Analysis of Maneuver Optimization Strategies," *AAS/AIAA Astrodynamics Specialist Conference*, Kalispell, Montana, AAS 87-486 (August1987).

[8] Rush, B., Owen, W.M., Bhaskaran, S., and Synnott, S.P., "Optical Navigation for the EPOXI Mission," in *Advances in the Astronautical Sciences*, Vol. 140, P. 1669. 21st AAS/AIAA Space Flight Mechanics Conference, New Orleans, Louisiana, February 13 to 17, 2011.

[9] P. E. Gill, W. Murray, and M. A. Saunders, *User's Guide for SNOPT Version 7: Software for Large-Scale Nonlinear Programming*, June 16, 2008 (PDF available from http://ccom.ucsd.edu/~peg/Software.html).